Uncertainty Analysis of Thermal Transmission Properties Determined by ASTM C 177

Robert R. Zarr[1]

Abstract:

An uncertainty analysis for steady-state thermal transmission properties determined by the National Institute of Standards and Technology (NIST) 1016 mm Guarded-Hot-Plate apparatus is presented for fibrous-glass blanket and expanded polystyrene board. The uncertainties are presented for the guarded-hot-plate apparatus in the single-sided mode of operation covering specimen heat flows from 0.5 W to 5 W. The relative expanded uncertainties for thermal resistance increase from 1 % to 3.5 % for thicknesses of 25.4 mm to 254 mm, respectively. Although these uncertainties have been developed for two thermal insulation materials, the results are indicative of other insulation materials measured at a mean temperature near 297 K (23.9 °C). This assessment of uncertainties is of particular interest for users of Test Method C 177 that operate similar apparatus at low heat flows (i.e., near or less than 1 W). Implications for laboratories that develop secondary standards from NIST calibrations are discussed.

Keywords: building technology; calibration; expanded polystyrene board; fibrous glass blanket; guarded hot plate; heat flow; thermal conductivity; thermal insulation; thermal resistance; standard uncertainty; expanded uncertainty

[1] Mechanical Engineer, Building and Fire Research Laboratory, National Institute of Standards and Technology, Gaithersburg, Maryland 20899-8632 USA

Introduction

The accurate determination of steady-state thermal transmission properties for building materials, especially thermal insulation, is important for determining the heat transmission through the thermal envelope of buildings and for subsequently sizing the conditioning equipment necessary to control the thermal environment of the building space. Recent renewed interest in energy efficiency in buildings has resulted in manufacturers producing higher performance thermal insulation materials and, consequently, requiring thicker reference materials. The National Institute of Standards and Technology (NIST) provides certified reference materials, such as NIST thermal insulation Standard Reference Materials (SRMs®) and Calibrated Transfer Specimens (CTS), using the guarded-hot-plate method.

The guarded-hot-plate method, which was standardized in 1945 after many years of effort and designated ASTM Test Method C 177 [1], has become an authoritative measurement technique in North America. Thermal insulation reference materials having certified values of thermal resistance are used by laboratories for checking the operation of guarded-hot-plate apparatus (Test Method C 177) and for the calibration of heat-flow-meter apparatus (ASTM Test Method C 518 [2]). In many cases, these laboratories utilize NIST certified reference materials to develop secondary standards for use as part of their quality control and assurance processes. Of interest to both NIST and industry is the development of valid uncertainty statements for NIST certified reference materials.

In October 1992, NIST officially adopted a new policy [3] for the expression of measurement uncertainty consistent with international practices. The NIST policy is based on recommendations by the Comité International des Poids et Mesures (CIPM) given in the *Guide to the Expression of Uncertainty in Measurement* [4] or "GUM" as it is now often called. Based on the approach advocated in the GUM, an uncertainty (re-)assessment of the NIST 1016 mm Guarded-Hot-Plate

apparatus was recently published for a specific low-density fibrous-glass blanket at thicknesses from 25.4 mm to 228.6 mm at a mean temperature of 297 K [5].

This paper extends the results by including additional types of fibrous-glass blanket insulations as well as expanded polystyrene board and a composite polystyrene board. Firstly, this paper describes the thermal transmission properties defined in ASTM C16 standards, the measurement principle for double- and single-sided operation configurations, and experimental results for the NIST 1016 mm Guarded-Hot-Plate apparatus. There is a description of the measurement uncertainty based on the GUM approach that includes definitions of terms, sources of uncertainty, and quantification of uncertainty components for the NIST 1016 mm Guarded-Hot-Plate apparatus. Lastly, the paper presents a discussion of the measurement uncertainty for the apparatus and the implications for users of Test Method C 177.

Thermal Transmission Properties

Test method C 177 is considered an absolute measurement procedure because the resulting thermal transmission properties are determined directly from basic measurements of length, area, temperature, and electrical power. That is, the test results are not determined by ratio of quantities as is the case for Test Method C 518, for example. Essentially, the method establishes steady-state heat flow through flat homogeneous slabs – the surfaces of which are in contact with adjoining parallel boundaries (i.e., plates) maintained at constant temperatures. The steady-state heat transmission properties of the test specimen are determined using Fourier's heat conduction equation by monitoring the boundary temperatures, plate separation, specimen heat flow, and knowing the geometric shape factor for heat flow. In principle, the method can be used over a wide range of building materials, mean temperatures, and temperature differences but, for this paper, the discussion

is limited to thermal insulations tested at a mean temperature of 297 K (23.9 °C) and a temperature difference less than 28 K.

ASTM Practice C 1045 [6] provides a uniform calculation procedure for thermal transmission properties of materials based on measurements from steady-state one dimensional methods such as ASTM Test Method C 177. Table 1 summarizes the generalized one-dimensional equations for thermal resistance (R), thermal conductance (C), thermal resistivity (r), and thermal conductivity (λ). Here, Q is the time-rate of one-dimensional heat flow through the meter area of the guarded-hot-plate apparatus; A is the meter area of the apparatus normal to the heat flow direction; ΔT is the temperature difference across the specimen; and, L is the specimen thickness.

Measurement Principle

A guarded-hot-plate apparatus (that has appropriate plate temperature controllers) can be operated in either a double-sided mode or in a single-sided mode (also known as two-sided or one-sided mode, respectively) as illustrated in Fig. 1. Figure 1 shows the essential features of a guarded-hot-plate apparatus designed for operation near ambient temperature with the plates in a horizontal configuration and heat flow (Q) in the vertical direction through the specimens. In principle, both modes of operation are covered in Test Method C 177; however, additional information on the single-sided mode is available in ASTM Practice C 1044 [7]. For completeness, this report presents both modes of operation but only the single-sided mode is examined in the uncertainty analysis.

Double-sided Mode

In the double-sided mode of operation (Fig. 1a), two specimens having nearly the same density, size, and thickness are placed on either surface of the guarded hot plate and clamped securely by the cold plates. Under ideal conditions, the guarded hot plate and the cold plates provide constant-

temperature boundary conditions to the specimen surfaces and lateral heat flows (Q_{gap} and Q_{edge}) and their effects are reduced to negligible proportions with proper guarding. Thus, under steady-state conditions, the apparatus provides one-dimensional heat flow (Q) normal to the meter area of the specimen pair. Typically, secondary guarding is provided by a chamber enclosure that conditions the air surrounding the plates to a temperature near the mean specimen temperature (that is, the average surface temperatures of the hot and cold plates in contact with the specimens).

Under steady-state conditions, the operational definition [6] for the mean (apparent) thermal conductivity[2] of the specimen pair (λ_{exp}) is

$$\lambda_{exp} = \frac{Q}{A[(\Delta T / L)_1 + (\Delta T / L)_2]} \tag{1}$$

where $(\Delta T / L)_1$ is the ratio of the surface-to-surface temperature difference ($T_h - T_c$) to the thickness (L) for Specimen 1. A similar expression is used for Specimen 2.

For experimental situations where the temperature differences and the specimen thicknesses are nearly the same, respectively, Equation (1) is reduced to

$$\lambda_{exp} = \frac{Q L_{average}}{2 A \Delta T_{average}} \tag{2}$$

Using the relationship from Table 1, Equation (2) can be rewritten to determine the thermal resistance of the specimen pair.

$$R = \frac{2A(\Delta T)}{Q} \tag{3}$$

In the double-sided mode of operation, the thermal transmission properties correspond to a mean

---

[2] The thermal transmission properties of heat insulators determined from standard test methods typically include several mechanisms of heat transfer, including conduction, radiation, and possibly convection. For that reason, some experimentalists will include the adjective "apparent" when describing thermal conductivity of thermal insulation. However, for brevity, the term thermal conductivity will be used in this paper.

specimen temperature T_m given by $T_m = (T_h + T_c)/2$.

Single-sided Mode

In the single-sided mode of operation (Fig. 1b), auxiliary thermal insulation is placed between the hot plate and the auxiliary cold plate. The auxiliary cold plate and the hot plate are maintained at essentially the same temperature and the heat flow (Q') through the auxiliary insulation is calculated as follows [7]:

$$Q' = C'A(T_h - T_c') \approx 0 \tag{4}$$

where the prime ($'$) notation denotes a quantity associated with the auxiliary thermal insulation and C' is the thermal conductance of the auxiliary insulation. As noted in Fig. 1b, the temperature of the hot surface is assumed to be uniform and, hence, $T_h = T_h' = T_c'$ In practice, however, $T_h \approx T_h' \approx T_c'$ and $Q' \approx 0$. The specimen heat flow (Q) is computed in the following equation:

$$Q = Q_m - Q' \tag{5}$$

where Q_m is the power input to the meter plate. In the single-sided mode, the factor 2 is removed from Equations (2) and (3) as shown in Equations (6) and (7), respectively.

$$\lambda_{exp} = \frac{QL_{average}}{A\Delta T_{average}} \tag{6}$$

$$R = \frac{A(\Delta T)}{Q} \tag{7}$$

Experimental Results

This study investigated the following types of thermal insulation materials – fibrous-glass blanket, expanded polystyrene board, and a composite board. The fibrous-glass blanket materials were obtained from five different sources (designated Materials 1-5) and covered a range of bulk

densities (ρ) from 6.2 kg·m^{-3} to 16 kg·m^{-3} and thicknesses (L) from 25.4 mm to 254 mm. Specimens

of expanded polystyrene board (Material 6) covered a range of bulk densities from 37 kg·m^{-3} to

43 kg·m^{-3} and nominal thicknesses from 25 mm to 100 mm. Material 7 was a composite material

(115 kg·m^{-3}, 110 mm thick,) consisting of a core of expanded polystyrene board and one layer of

plastic cladding on each specimen surface.

The NIST 1016 mm Guarded-Hot-Plate apparatus, illustrated in Fig. 2, has been described

previously [5] and is discussed briefly here.   The apparatus plates (shown in a horizontal

configuration in Fig. 2) were fabricated from 6061-T6 aluminum and the plate surfaces in contact

with the specimens were anodized black to have a total emittance of 0.89.   The diameters of the

meter plate and guard plate are nominally 0.4064 m and 1.016 m, respectively for a guard-to-meter

ratio of 2.5.

The guarded-hot-plate measurements were conducted at a mean temperature (T_m) of 297 K and

a ΔT of either 22.2 K or 27.8 K. The apparatus was operated in the single-sided mode of operation

(Fig. 1b) with heat flow in the vertical direction utilizing a 100 mm thick specimen of expanded

polystyrene foam as the auxiliary insulation. Table 2 summarizes the input estimates for 16 sets of

data for ρ, L, Q, A, ΔT and the output estimates (that is, the thermal transmission data) for R and λ

for Materials 1-7. The uncertainty assessment for the measurements is developed and discussed

below.

Measurement Uncertainty

The combined standard uncertainty $u_c(y)$ of a measurement result y is expressed as the positive

square root of the combined variance $u_c^2(y)$ [3-4]:

$$u_c(y) = \sqrt{\sum_{i=1}^{N} c_i^2 u^2(x_i)} . \tag{8}$$

where the quantity y is a function of the independent parameters x_i : $y = f(x_1, x_2, ... x_N)$. Equation (8) is commonly referred to as the "*law of propagation of uncertainty*" or the "root-sum-of-squares." The sensitivity coefficients (c_i) are equal to the partial derivative of the function f with respect to an input quantity ($\partial f/\partial X_i$) evaluated for the input quantity equal to an input estimate ($X_i = x_i$). The corresponding term, $u(x_i)$, is the standard uncertainty associated with the input estimate x_i. The relative combined standard uncertainty is defined as follows (where $y \neq 0$):

$$u_{c,r}(y) = \frac{u_c(y)}{|y|} .$$

(9)

Following the approach given in the GUM, each $u(x_i)$ is evaluated as either a Type A or a Type B standard uncertainty, or both. Type A standard uncertainties are evaluated by statistical means. The evaluation of uncertainty by means other than a statistical analysis of a series of observations is termed a Type B evaluation [3]. Type B evaluations are usually based on scientific judgment and may include measurement data from another experiment, experience, a calibration certificate, manufacturer specification, or other means as described in References [3-4].

It should be emphasized that the designations "A" and "B" apply to the two different methods of evaluation, *not* the type of error. In other words, the designations "A" and "B" have nothing to do with the more traditional terms "random" or "systematic." Categorizing the evaluation of uncertainties as Type A or Type B is a matter of convenience, since both are based on probability distributions[3] and are combined equivalently. Thus, Equation (8) can be expressed in simplified form as:

$$u_c = \sqrt{u_A^2 + u_B^2} .$$

(10)

Combined Standard Uncertainty for R

The application of Equation (8) to the equation for R given in Table 1 yields the following expression for the combined standard uncertainty of R:

$$u_c(R) = \sqrt{\left(\frac{\Delta T}{Q}\right)^2 u^2(A) + \left(\frac{A}{Q}\right)^2 u^2(\Delta T) + \left(\frac{-A(\Delta T)}{Q^2}\right)^2 u^2(Q)}. \tag{11}$$

Strictly speaking, the sensitivity coefficients c_A, $c_{\Delta T}$, and c_Q given in Equation (11) are evaluated for the input estimates of A, ΔT and Q. However, treating the sensitivity coefficients as continuous mathematical functions provides insightful information on the measurement uncertainty for R (as will be shown later). From Equation (11), it is evident that as Q decreases, the sensitivity coefficients c_A, $c_{\Delta T}$, and c_Q increase.

The relative standard uncertainty for R is determined by dividing Equation (11) by R.

$$u_{c,r} = \frac{u_c(R)}{R} = \sqrt{\left(\frac{u(A)}{A}\right)^2 + \left(\frac{u(\Delta T)}{\Delta T}\right)^2 + \left(\frac{u(Q)}{Q}\right)^2} \tag{12}$$

Equation (12) expresses the standard uncertainties in relative terms and, thus, is generally more convenient for determining the relative standard uncertainty, given fixed-value input estimates. However, as will be shown later, Equation (12) can provide incomplete results if the single-point estimates are assumed to apply over the entire range of apparatus operation (i.e., for different levels of specimen heat flow).

Combined Standard Uncertainty for λ

In general, NIST provides value assignments and uncertainties for R. For completeness in this paper, the application of Equation (8) to the equation for λ given in Table 1 yields the following expression for the combined standard uncertainty of λ:

---

[3] Note that the probability distribution for a Type B evaluation, in contrast to a Type A evaluation, is assumed based on the experimenter's judgment.

$$u_c(\lambda) = \sqrt{\left(\frac{L}{A(\Delta T)}\right)^2 u^2(Q) + \left(\frac{Q}{A(\Delta T)}\right)^2 u^2(L) + \left(\frac{-QL}{A^2(\Delta T)}\right)^2 u^2(A) + \left(\frac{-QL}{A(\Delta T)^2}\right)^2 u^2(\Delta T)} \quad (13)$$

One of the major differences between the uncertainties computed in Equations (11) and (13) is the inclusion of specimen thickness (*L*) for λ (Table 1). If the uncertainty in *L* is large, the uncertainty in λ will be greater than the uncertainty for *R*, all other factors the same. Otherwise, for small values of *u(L)*, the relative uncertainties for *R* and λ are nearly the same. The relative standard uncertainty for λ is determined by dividing Equation (13) by λ.

$$u_{c,r} = \frac{u_c(\lambda)}{\lambda} = \sqrt{\left(\frac{u(Q)}{Q}\right)^2 + \left(\frac{u(L)}{L}\right)^2 + \left(\frac{u(A)}{A}\right)^2 + \left(\frac{u(\Delta T)}{\Delta T}\right)^2} \quad (14)$$

Expanded Uncertainty

The expanded uncertainty, *U*, is obtained by multiplying the combined standard uncertainty, $u_c(y)$, by a coverage factor, *k* when an additional level of uncertainty is required that provides an interval (similar to a confidence interval, for example):

$$U = ku_c(y) = k\sqrt{\sum c_i^2 u^2(x_i)_A + \sum c_i^2 u^2(x_i)_B} \ . \quad (15)$$

The value of *k* is chosen based on the desired level of confidence to be associated with the interval defined by *U* and typically ranges from 2 to 3. Under a wide variety of circumstances, a coverage factor of *k* = 2 defines an interval having a level of confidence of about 95 % and *k* = 3 defines an interval having a level of confidence greater than 99 %. At NIST, a coverage factor of *k* = 2 is used, by convention [3]. The relative expanded uncertainty, U_r, is defined as follows (where *y* ≠ 0):

$$U_r = \frac{U}{|y|} \ . \quad (16)$$

Sources of Uncertainty

Table 3 presents a comprehensive, but not exhaustive, list of uncertainty sources for single-sided measurements of λ for the NIST 1016 mm Guarded-Hot-Plate apparatus. The uncertainty sources can be classified in one of the following specialist areas of metrology– dimensional for the meter area (A) and thickness (L); temperature for ΔT; and, electrical for voltage and resistance measurements. The uncertainty assessment due to parasitic heat flows (ΔQ) requires either heat-transfer analyses or additional experiments, or both. It should be noted that the list presented in Table 3 is unique for the NIST 1016 mm Guarded-Hot-Plate apparatus and should only be used as a guide for other apparatus.

Quantification of Uncertainty Components

A useful approach taken in this paper is to treat each uncertainty component separately and evaluate the uncertainty component as either a Type A or Type B standard uncertainty [3-4]. Detailed procedures for quantifying the contributory uncertainties for components $u(A)$, $u(L)$, $u(\Delta T)$, and $u(Q)$ have been described in Reference [5] and, therefore, are only discussed briefly here for the first row of data given in Table 2.

Meter Area (A)

The meter area is the mathematical area through which the heat input to the meter plate (Q) flows normal to the heat-flow direction under ideal guarding conditions into the specimen. Test Method C 177 [1] defines the meter area as the sum of the surface area of the meter plate and one-half the surface area of the guard gap. Based on this definition, and including thermal expansion effects, the circular meter area was calculated from Equation (17) below [5]:

$$A = \frac{\pi}{2}\left(r_o^2 + r_i^2\right)\left(1 + \alpha\,\Delta T_{mp}\right)^2 \tag{17}$$

where:

r_o = outer radius of meter plate (m) = 0.20282 m;

r_i = inner radius of guard plate (m) = 0.20371 m;

α = coefficient of thermal expansion of 6061-T6 aluminum (K^{-1}) = 23.6×10^{-6} K^{-1}; and,

ΔT_{mp} = temperature difference of the meter plate from the temperature at which r_0 and r_i were

measured (K) = $T_h - 20$ °C.

The application of Equation (8) to Equation (17) yields

$$u_c(A) = \sqrt{c_{r_0}^2 u^2(r_o) + c_{r_i}^2 u^2(r_i) + c_\alpha^2 u^2(\alpha) + c_{\Delta T_{mp}}^2 u^2(\Delta T_{mp})} \tag{18}$$

with

$$c_{r_o} = \partial A/\partial r_o = \pi r_o (1 + \alpha \Delta T_{mp})^2$$

$$c_{r_i} = \partial A/\partial r_i = \pi r_i (1 + \alpha \Delta T_{mp})^2$$

$$c_\alpha = \partial A/\partial \alpha = \pi \Delta T_{mp} (r_o^2 + r_i^2)(1 + \alpha \Delta T_{mp})$$

$$c_{\Delta T_{mp}} = \partial A/\partial(\Delta T_{mp}) = \pi \alpha (r_o^2 + r_i^2)(1 + \alpha \Delta T_{mp})$$

For (T_h) maintained at 308 K (35 °C), the meter area (A) was computed to be 0.12989 m^2. The combined standard uncertainty $u_c(A)$ and relative standard uncertainty $u_{c,r}(A)$ were determined to be 2.47×10^{-5} m^2 and 0.019 %, respectively. The value for $u_c(A)$ is quite small near ambient temperature but increases as T_h departs from ambient conditions.

Thickness (L)

The standard uncertainty for thickness is required only for Equations (13) and (14). In the single-sided mode of operation, the in-situ thickness of the specimen (Figure 2) is monitored during a test by averaging four linear position transducers attached to the periphery of the cold plate at approximate 90° intervals. For compressible fibrous-glass blanket specimens (Materials 1-

5), the plate separation is maintained by four fused-quartz spacers placed at the periphery of the specimen at the same angular intervals as the four linear position transducers. For the semi-rigid specimens (Materials 6-7) the plate separation is maintained by the specimen. The combined standard uncertainty for L is given by

$$u_c(L) = \sqrt{u^2(L_1) + u^2(L_2) + u^2(L_3) + u^2(L_4) + u^2(L_5)} \qquad (19)$$

where the sensitivity coefficients are equal to unity ($c_{L_i} = 1$) and the contributory uncertainties from Table 3 are

$u(L_1)$ = standard uncertainty of the in-situ linear position measurement (m);

$u(L_2)$ = standard uncertainty of the fused-quartz spacer length (m);

$u(L_3)$ = standard uncertainty of the repeatability of the linear position measurement (m);

$u(L_4)$ = standard uncertainty of the plate flatness (m); and,

$u(L_5)$ = standard uncertainty of the cold plate deflection under axial loading (m).

The contributory uncertainties $u(L_i)$ are discussed in detail in Reference [5] and are summarized here; values for $u(L_{1,2,3,4,5})$ (for Table 2, row 1) are 20 μm, 1.9 μm, 6.4 μm, 7.9 μm, and 31 μm, respectively. For $L = 25.4$ mm, $u_c(L)$ is 38 μm and $u_{c,r}(L)$ is 0.15 %. Note that at greater specimen thicknesses, values of $u_{c,r}(L)$ decrease substantially as L increases.

Temperature Difference (ΔT)

The primary plate temperatures (T) are determined by computing temporal averages of 240 observations over a steady-state interval of 4 h for three small capsule platinum resistance thermometers (PRTs). The combined standard uncertainty for T (Table 3) is given by Equation (20)

$$u_c(T) = \sqrt{u^2(T_1) + u^2(T_2) + u^2(T_3)} \qquad (20)$$

where the sensitivity coefficients are equal to unity ($c_{T_i} = 1$) and the contributory uncertainties from

Table 3 are

$u(T_1)$ = standard uncertainty for the measurement of T_h, T_c (K);

$u(T_2)$ = calibration of the PRTs (K); and,

$u(T_3)$ = miscellaneous contributory uncertainties identified in Table 3.

The dominant contributory uncertainty for $u(T_1)$ is the Type B evaluation for the electrical

resistance measurement (in ohms) of the PRTs. The evaluation assumes a uniform distribution

having an interval $2a$ [3-4] where a was determined from the manufacturer specification for the

digital multimeter (DMM). For a equal to 0.039 Ω for the 300 Ω DMM range, u_B is 0.022 Ω

($a/\sqrt{3}$), which when propagated in the calibration curve fit yields a value of 0.058 K. Combining

this value and the Type A evaluation for regression analysis of 0.0052 K yields $u(T_1)$ of 0.058 K.

The estimated values for $u(T_2)$ and $u(T_3)$ are 0.005 K and 0.019 K, respectively [5]. Substituting

in Equation (20), $u_c(T)$ is 0.061 K.

From Equation (1), ΔT is equal to the difference of T_h minus T_c. Applying Equation (8) and

setting $u_{T_h} = u_{T_c} = u_T$ gives Equation (21):

$$u_c(\Delta T) = \sqrt{u_{T_h}^2 + u_{T_c}^2} = \sqrt{2u_T^2} \tag{21}$$

Substitution of $u_c(T) = 0.061$ K into Equation (21) yields a value for $u_c(\Delta T)$ of 0.086 K. For ΔT of

22.2 K and 27.8 K, $u_{c,r}(\Delta T)$ is 0.39 % and 0.31 %, respectively. Note that the value for $u_c(\Delta T)$ of

0.086 K was used in the uncertainty assessment for $u_c(A)$ in Equation (18).

Heat Flow (Q)

The specimen heat flow (Q) is evaluated as the difference between the power input to the meter

plate (Q_m) and corrections for any parasitic heat losses across the guard gap (Q_{gap}), edge effects

(Q_ε) and auxiliary heat flow (Q'). Under ideal conditions, lateral heat flows (Q_{gap}, Q_ε) and the

auxiliary heat flow (Q') computed in Equation (4) are reduced to negligible proportions with proper guarding and operation. Although the parasitic heat flows are reduced under steady-state conditions to very small values (on the order of 1 mW, or less), the uncertainty associated with each term can be large as shown in Reference [5]. Essentially, the contributory uncertainties $u(Q_{gap})$, $u(Q_\varepsilon)$, and $u(Q')$ can be estimated as Type B components either from theoretical calculations (with some difficulty due to the mathematics) or, in this case, from empirical data from other experiments described in detail in Reference [5].

The combined standard uncertainty for Q (Table 3) is given by Equation (22)

$$u_c(Q) = \sqrt{u^2(Q_m)_A + u^2(Q_m)_B + u_c^2(\Delta Q)} \qquad (22)$$

where the sensitivity coefficients are equal to unity and the contributory uncertainties are

$u(Q_m)_A$ = Type A component – repeated observations ($n = 240$) during a test (W);

$u(Q_m)_B$ = Type B component of the meter-plate power input (W); and,

$u_c(\Delta Q)$ = combined standard uncertainty for parasitic heat flows (Q_{gap}, Q_ε, and Q') (W).

At L equal to 25.4 mm, the values for $u(Q_m)_A$, $u(Q_m)_B$, and $u_c(\Delta Q)$ are 0.0006 W, 0.0016 W, and 0.0087 W, respectively. The dominant uncertainty source is the uncertainty in the parasitic heat flows which, in turn, is due primarily to the uncertainty in the gap thermopile voltage and temperature difference across the auxiliary insulation [5]. For Q equal to 5.113 W, the relative combined standard uncertainty $u_{c,r}(Q)$ is 0.17 % but increases considerably with specimen thickness.

Discussion

Thermal Resistance (*R*)

The standard uncertainties for the input estimates Q, A, and ΔT given in Table 2 are summarized in Table 4 for R. Across the 16 sets of data given in Table 4, the standard uncertainties are relatively constant. The values for $u(Q)$ range from 8 mW to 9 mW; the value for $u(A)$ is about 2.5×10^{-5} m^2; and for $u(\Delta T)$ about 0.09 K. Table 4 also summarizes the corresponding sensitivity coefficients c_Q, c_A, and $c_{\Delta T}$, the combined standard uncertainty $u_c(R)$, and expanded uncertainty $U(R)$ determined from Equations (11) and (15), respectively. Values of $U(R)$ having a coverage factor of $k = 2$ range from 0.0048 m^2·K·W^{-1} to 0.19 m^2·K·W^{-1}. For convenience, the *relative* expanded uncertainties (Table 4) when reported to customers, are rounded to the next highest 0.5 %, yielding a range for $U_r(R)$ from 1 % to 3.5 %.

To gain insight on their relative contributions, Fig. 3 plots the absolute value of the sensitivity coefficients times their respective standard uncertainties, in m^2·K·W^{-1}, as a function of specimen heat flow (Q) in watts. The measurement data given in Table 4 are plotted as symbols identifying the Materials 1-7. The theoretical curves from Equation (11) for $|c_Q \cdot u(Q)|$, $|c_{\Delta T} \cdot u(\Delta T)|$, and $|c_A \cdot u(A)|$ are shown as solid, dashed, and dotted lines, respectively. At heat flows above 2.5 W, the uncertainty for ΔT is the dominant component. However, below 2 W and especially at 1 W and less, the uncertainty for Q is the dominant component. Moreover, because the sensitivity coefficient c_Q in Equation (11) is proportional to the inverse square of Q, and $u(Q)$ is always a non-zero value, the resulting effect on uncertainty of R will be substantial at low specimen heat flows.

Figure 4 plots the data for $U(R)$ in m^2·K·W^{-1} from Table 4 as a function of specimen heat flow, Q in watts and specimen heat flux (Q/A) in W·m^{-2}. Materials 1-7 are identified by separate symbols for fibrous glass blanket; expanded polystyrene board; and the composite board. Using Equation (11), predicted curves for $U(R)$ are shown for a fixed value of A of 0.12989 m^2, ΔT of 22 K and 28 K, and Q varying from 0.6 W to 5.1 W. For 25 mm thick specimens, the values of Q are relatively high,

near 4 W to 5 W, and the corresponding relative expanded uncertainty is low (less than 0.007 $m^2 \cdot K \cdot W^{-1}$, or 1 %). As the specimen thickness increases, however, Q decreases and $U(R)$ dramatically increases due to the effects discussed above in Fig. 3. Furthermore, the graph illustrates that for any non-zero value for $u(Q)$ (and to a lesser extent for $u(A)$ and for $u(\Delta T)$), the expanded uncertainty will increase substantially at low values of specimen heat flow (Q).

Thermal Conductivity (λ)

A similar summary of data is given in Table 5 which includes the same standard uncertainties for Q, A, and ΔT given in Table 4 and also includes the standard uncertainty for the input estimates for L given in Table 2. As was the case for $u(Q)$, $u(A)$, and $u(\Delta T)$, the standard uncertainties for $u(L)$ across the measurements are also relatively constant, ranging from 3×10^{-5} mm to 4×10^{-5} mm. Table 5 also summarizes the corresponding sensitivity coefficients c_L, c_Q, c_A, and $c_{\Delta T}$ (Equation (13)), the combined standard uncertainty $u_c(\lambda)$, and expanded uncertainty $U(\lambda)$ determined using Equations (13) and (15), respectively. Values of $U(\lambda)$, having a coverage factor of $k = 2$, range from 0.00041 $W \cdot m^{-1} \cdot K^{-1}$ to 0.014 $W \cdot m^{-1} \cdot K^{-1}$.

Figure 5 plots the data for $U(\lambda)$ in $W \cdot m^{-1} \cdot K^{-1}$ from Table 5 as a function of specimen heat flow, Q in watts and specimen heat flux (Q/A) in watts per square meter. Materials 1-7 are identified by the same unique symbols illustrated in Fig. 3 and 4. Like Figure 4, values of $U(\lambda)$ for the different materials increase as Q decreases from 5.1 W to 0.6 W. Using Equation (13), parametric curves of $U(\lambda)$ for L from 25.4 mm to 254 mm, fixed value of A of 0.12989 m^2, and ΔT of 22 K or 28 K are shown as either solid or dashed lines, respectively. Note that these curves are theoretical and may not represent any actual material over portions of a particular curve. The plot shows how a small increase in ΔT from 22 K to 28 K can lower the uncertainty for λ (as also evident in Equation (13)).

The results from Figures 3-5 strongly suggest that, for the materials studied, the expanded

uncertainty is independent of material. The primary factor in determining the measurement uncertainty is the relative contributions from the products of variances and their respective sensitivity coefficients. For thin specimens near 25.4 mm, values of Q range from 3 W to 5 W and the major contribution in uncertainty is due to the thickness measurement. As specimen thickness is increased, the specimen heat flow decreases. At specimen heat flows near 1 W or less, the major contribution is due to the uncertainty in determining the specimen heat flow.

Measurement Uncertainty, Precision, and Bias

The term "measurement uncertainty" should not be confused with the ASTM definitions for the terms "precision and bias." Strictly speaking, measurement uncertainty is applicable to the test results from an individual laboratory. It follows that the assessment presented herein is applicable only to the NIST 1016 mm Guarded Hot Plate apparatus, although the approach can be used as a guide for other laboratories. In contrast, precision and bias are defined from a classical approach that distinguishes between random and systematic effects. Precision is defined as the closeness of agreement between independent test results under stipulated conditions and may include within-laboratory (repeatability) and between-laboratory (reproducibility) components [8]. Bias is defined as the difference between the expectation of the test results and the accepted reference value [8]. Precision and bias statements, as defined by ASTM, are obtained ideally from the results of an interlaboratory comparison [9] described in Practice E 691 [10]. Thus, the ASTM terms precision and bias apply only to an ASTM test method (such as Test Method C 177) and are to be used for guidance purposes only [11].

Metrological Traceability

As part of its policy on traceability, NIST has adopted the definition of traceability provided in the most recent version of the *International Vocabulary of Basic and General Terms in Metrology*

[12]. Metrological traceability is defined as a "property of the result of a measurement or the value of a standard whereby it can be related to stated references, usually national or international standards, through an unbroken chain of comparisons all having *stated uncertainties*." "Stated uncertainties" must be evaluated and expressed in accordance with the GUM (as shown in this paper and Reference [5]). The recipients of NIST certified reference materials must determine how to incorporate the specified uncertainty in their measurement processes as part of the metrological traceability chain. It is important for the user to note that measurement uncertainty inevitably increases along a sequence of calibration measurements.

Conclusions

Standard and expanded uncertainties for thermal resistance (R) and thermal conductivity (λ) for the NIST 1016 mm Guarded-Hot-Plate apparatus are reported in a format consistent with current NIST policy on the international expression of measurement uncertainty. The uncertainty assessment investigated three types of thermal insulation materials – fibrous-glass blanket, expanded polystyrene board, and a composite board. Steady-state thermal transmission properties of the materials were determined at a mean temperature near 297 K using a guarded-hot-plate apparatus operated in the single-sided mode of operation over a range of heat flows (Q) from 0.5 W to 5 W.

The results of the study strongly suggest that, for the materials studied, the expanded uncertainty is independent of material. Further, it is insufficient to provide only a single value for uncertainty, particularly when using the guarded-hot-plate apparatus over a wide range of specimen heat flows. In this case, the relative expanded uncertainties for thermal resistance increase from 1 % for a thickness of 25.4 mm to 3.5 % for a thickness of 254 mm. The increase in uncertainty is non-linear

as the specimen heat flow decreases and is particularly important at values of Q near or less than 1 W.

It is important to note that, because of the nature of uncertainty propagation as shown in Equation (8), the measurement uncertainty increases along a calibration hierarchy. That is, a metrological traceability chain (from NIST to a customer) is defined through a sequence of calibrations (starting from a stated reference to the final measuring instrument). Taken together with the results of Figures 3-5, this effect may have considerable implications for the insulation industry and thermal testing communities in reliably evaluating the thermal performance of thick specimens of thermal insulation (i.e., at low heat flows).

The uncertainty assessment procedure presented here is also helpful for users of Test Method C 177 as a guide in assessing their measurement uncertainty. It is suggested that Subcommittee C16.30 on Thermal Measurements consider this assessment as an example for possible inclusion in Test Method C 177 as a user template. Finally, it should be noted that the uncertainty analysis approach advocated in the GUM is, in principle, applicable to any quantitative measurement process and, therefore, applicable to other ASTM test methods, as well.

References

[1] ASTM Standard C177-04: Standard Test Method for Steady-State Heat Flux Measurements and Thermal Transmission Properties by Means of the Guarded-Hot-Plate Apparatus, *Annual Book of ASTM Standards*, ASTM International, West Conshohocken, PA 2008.

[2] ASTM Standard C518-04: Standard Test Method for Steady-State Thermal Transmission Properties by Means of the Heat Flow Meter Apparatus, *Annual Book of ASTM Standards*, ASTM International, West Conshohocken, PA 2008.

[3] Taylor, B.N. and C.E. Kuyatt, "Guidelines for Evaluating and Expressing the Uncertainty of NIST Measurement Results," *NIST Technical Note 1297, 1994 Edition*.

[4] ISO, "Guide to the Expression of Uncertainty in Measurement," International Organization for Standardization, Geneva, Switzerland, 1993.

[5] Zarr, R. R., "Assessment of Uncertainties for the NIST 1016 mm Guarded-Hot-Plate Apparatus: Extended Analysis for Low-Density Fibrous-Glass Thermal Insulation," NIST Technical Note 1606, February 2009.

[6] ASTM Standard C1045-07: Standard Practice for Calculating Thermal Transmission Properties Under Steady-State Conditions, *Annual Book of ASTM Standards*, ASTM International, West Conshohocken, PA 2008.

[7] ASTM Standard C1044-07: Standard Practice for Using a Guarded-Hot-Plate Apparatus or Thin-Heater Apparatus in the Single-Sided Mode, *Annual Book of ASTM Standards*, ASTM International, West Conshohocken, PA 2008.

[8] ASTM Standard E456-08e1: Standard Terminology for Relating to Quality and Statistics, *Annual Book of ASTM Standards*, ASTM International, West Conshohocken, PA 2008.

[9] ASTM Standard E 1488-08a: Standard Guide for Statistical Procedures to Use in Developing and Applying Test Methods, *Annual Book of ASTM Standards*, ASTM International, West Conshohocken, PA 2008.

[10] ASTM Standard E 691-08: Standard Practice for Conducting an Interlaboratory Study to Determine the Precision of a Test Method, *Annual Book of ASTM Standards*, ASTM International, West Conshohocken, PA 2008.

[11] Ullman, N. R., "Statistics in Developing and Using Test Methods: E 1488 Provides Guidance," *ASTM Standardization News*, Nov. 1997, pp. 28-33.

[12] "International Vocabulary of Basic and General Terms in Metrology (VIM)," BIPM, IEC, IFCC, ISO, IUPAC, IUPAP, OIML, 2nd ed., 1993, definition 6.10.

Tables

TABLE 1 – *Steady-State One-Dimensional Thermal Transmission Property Equations*

	Thermal Resistance R, m²·K·W⁻¹	Thermal Conductance C, W·m⁻²·K⁻¹	Thermal Resistivity r, m·K·W⁻¹	Thermal Conductivity λ, W·m⁻¹·K⁻¹
Equation	$R = \dfrac{A\Delta T}{Q}$	$C = \dfrac{Q}{A\Delta T}$	$r = \dfrac{A\Delta T}{QL}$	$\lambda = \dfrac{QL}{A\Delta T}$
Relationships	$R = \dfrac{1}{C} = \dfrac{L}{\lambda}$	$C = \dfrac{1}{R} = \dfrac{\lambda}{L}$	$r = \dfrac{1}{\lambda}$	$\lambda = \dfrac{1}{r}$

TABLE 2 – *Guarded-Hot-Plate Thermal Transmission Data (T_m = 297K)*

Material[a]	ρ, kg·m⁻³	L, mm	Q, W	A, m²	ΔT, K	R, m²·K·W⁻¹	λ, W·m⁻¹·K⁻¹
1	9.3	25.41	5.113	0.12989	22.22	0.564	0.0450
1	8.9	76.22	1.792	0.12989	22.22	1.61	0.0473
1	9.5	152.4	0.871	0.12989	22.22	3.31	0.0460
1	8.7	228.6	0.607	0.12989	22.22	4.75	0.0481
2	8.3	50.79	2.546	0.12989	22.22	1.13	0.0448
3	16.2	76.19	1.489	0.12989	22.22	1.94	0.0393
2	8.1	101.6	1.323	0.12989	22.22	2.18	0.0466
2	7.6	152.4	0.924	0.12989	22.22	3.13	0.0488
2	8.0	203.2	0.682	0.12989	22.22	4.23	0.0480
4	13.6	228.6	0.493	0.12989	22.22	5.85	0.0390
5	6.2	254.0	0.732	0.12991	27.78	4.93	0.0515
6	39.4	24.98	3.908	0.12989	22.22	0.738	0.0338
6	37.1	23.84	4.077	0.12989	22.22	0.708	0.0337
6	42.8	49.64	1.955	0.12989	22.22	1.48	0.0336
6	42.5	99.54	0.971	0.12989	22.22	2.97	0.0335
7	115.	109.8	0.744	0.12989	22.22	3.88	0.0283

[a]1 = NIST fibrous-glass blanket (Calibrated Transfer Specimen Lot)
[a]2-5 = Fibrous-glass blanket (from different manufacturers), ordered by thickness (*L*)
[a]6 = Expanded polystyrene, molded beads
[a]7 = Composite board (expanded polystyrene, plastic facers)

TABLE 3 – *List of Uncertainty Sources for λ (NIST 1016 mm Guarded-Hot-Plate Apparatus)*

1) Meter area (A)
   a) Plate dimensions
   b) Thermal expansion effects

2) Thickness (L)
   a) In-situ linear position measurement system
      i) Multiple observations
      ii) System uncertainty
   b) Dimensions of fused-quartz spacers
      i) Repeated observations
      ii) Caliper uncertainty
   c) Short-term repeatability
   d) Plate flatness
      i) Repeated observations
      ii) Coordinate measuring machine (CMM) uncertainty
   e) Plate deflection under axial loading of cold plate

3) Temperature difference (ΔT)
   a) Measurement (T_h , T_c)
      i) Digital multimeter (DMM) uncertainty
      ii) Platinum Resistance Thermometer (PRT) regression analyses for calibration data
   b) Calibration of PRTs
   c) Miscellaneous sources
      i) Contact resistance
      ii) Sampling of planar plate temperature
      iii) Axial temperature variations

4) Heat flow (Q)
   a) Direct current power measurement (Q_m)
      i) Standard resistor calibration
      ii) Standard resistor drift
      iii) PRT power input
      iv) Voltage measurement
   b) Parasitic heat flows (ΔQ)
      i) Guard-gap (Q_{gap})
      ii) Auxiliary insulation (Q')
      iii) Edge effects (Q_ε)

TABLE 4 – *Standard Component Uncertainties, Sensitivities, Combined, and Expanded Uncertainties for R.*
The material parameters for each row are given in the corresponding row in Table 2.

Material[a]	$u(Q)$, W	$u(A)$, m^2	$u(\Delta T)$, K	c_Q, m$^2\cdot$K$\cdot$W^{-2}	c_A, K$\cdot$W^{-1}	$c_{\Delta T}$, m$^2\cdot$W^{-1}	$u_c(R)$, m$^2\cdot$K$\cdot$W^{-1}	$U_r(R)$, %
1	0.0089	2.47×10^{-5}	0.086	-0.110	4.345	0.0254	0.0024	0.9
1	0.0083	2.47×10^{-5}	0.086	-0.899	12.402	0.0725	0.0098	1.2
1	0.0087	2.47×10^{-5}	0.086	-3.807	25.520	0.1492	0.036	2.2
1	0.0083	2.47×10^{-5}	0.086	-7.822	36.580	0.2138	0.068	2.8
2	0.0077	2.47×10^{-5}	0.086	-0.445	8.728	0.0510	0.0056	1.0
3	0.0082	2.47×10^{-5}	0.086	-1.302	14.923	0.0872	0.013	1.3
2	0.0078	2.47×10^{-5}	0.086	-1.649	16.798	0.0982	0.015	1.4
2	0.0083	2.47×10^{-5}	0.086	-3.384	24.061	0.1406	0.031	2.0
2	0.0082	2.47×10^{-5}	0.086	-6.201	32.573	0.1904	0.053	2.5
4	0.0079	2.47×10^{-5}	0.086	-11.876	45.074	0.2635	0.097	3.3
5	0.0084	2.54×10^{-5}	0.087	-6.728	37.933	0.1774	0.059	2.4
6	0.0081	2.47×10^{-5}	0.086	-0.189	5.685	0.0332	0.0032	0.9
6	0.0080	2.47×10^{-5}	0.087	-0.174	5.451	0.0319	0.0031	0.9
6	0.0083	2.47×10^{-5}	0.087	-0.755	11.368	0.0665	0.0085	1.2
6	0.0080	2.47×10^{-5}	0.087	-3.062	22.887	0.1338	0.027	1.8
7	0.0086	2.47×10^{-5}	0.086	-5.222	29.889	0.1747	0.047	2.4

[a]1 = NIST fibrous-glass blanket (Calibrated Transfer Specimen Lot)

[a]2-5 = Fibrous-glass blanket (from different manufacturers), ordered by thickness (*L*)

[a]6 = Expanded polystyrene, molded beads

[a]7 = Composite board (expanded polystyrene, plastic facers)

TABLE 5 – *Standard Component Uncertainties, Sensitivities, Combined, and Expanded Uncertainties for λ.*
The material parameters for each row are given in the corresponding row in Table 2.

Material[a]	$u(L)$, mm	$u(Q)$, W	$u(A)$, m^2	$u(\Delta T)$, K	c_L, $W \cdot m^{-2} \cdot K^{-1}$	c_Q, $m^{-1} \cdot K^{-1}$	c_A, $W \cdot m^{-3} \cdot K^{-1}$	$c_{\Delta T}$, $W \cdot m^{-1} \cdot K^{-2}$	$u_c(\lambda)$, $W \cdot m^{-1} \cdot K^{-1}$	$U_r(\lambda)$, %
1	3.8×10^{-5}	0.0089	2.47×10^{-5}	0.086	1.7718	0.0088	-0.3467	-0.0020	0.00020	0.9
1	3.5×10^{-5}	0.0083	2.47×10^{-5}	0.086	0.6208	0.0264	-0.3643	-0.0021	0.00029	1.2
1	3.5×10^{-5}	0.0087	2.47×10^{-5}	0.086	0.3017	0.0528	-0.3539	-0.0021	0.00049	2.1
1	3.5×10^{-5}	0.0083	2.47×10^{-5}	0.086	0.2105	0.0792	-0.3704	-0.0022	0.00068	2.8
2	3.7×10^{-5}	0.0077	2.47×10^{-5}	0.086	0.8820	0.0176	-0.3449	-0.0020	0.00022	1.0
3	3.5×10^{-5}	0.0082	2.47×10^{-5}	0.086	0.5159	0.0264	-0.3026	-0.0018	0.00027	1.3
2	3.8×10^{-5}	0.0078	2.47×10^{-5}	0.086	0.4583	0.0352	-0.3584	-0.0021	0.00033	1.4
2	3.8×10^{-5}	0.0083	2.47×10^{-5}	0.086	0.3200	0.0528	-0.3754	-0.0022	0.00048	2.0
2	3.7×10^{-5}	0.0082	2.47×10^{-5}	0.086	0.2364	0.0704	-0.3698	-0.0022	0.00060	2.5
4	3.7×10^{-5}	0.0079	2.47×10^{-5}	0.086	0.1708	0.0792	-0.3006	-0.0018	0.00065	3.3
5	3.5×10^{-5}	0.0084	2.54×10^{-5}	0.087	0.2029	0.0704	-0.3967	-0.0019	0.00062	2.4
6	2.6×10^{-5}	0.0081	2.47×10^{-5}	0.086	1.3541	0.0087	-0.2604	-0.0015	0.00015	0.9
6	2.7×10^{-5}	0.0080	2.47×10^{-5}	0.087	1.4124	0.0083	-0.2592	-0.0015	0.00015	0.9
6	2.8×10^{-5}	0.0083	2.47×10^{-5}	0.087	0.6772	0.0172	-0.2588	-0.0015	0.00019	1.2
6	2.6×10^{-5}	0.0080	2.47×10^{-5}	0.087	0.3364	0.0345	-0.2578	-0.0015	0.00031	1.8
7	2.9×10^{-5}	0.0086	2.47×10^{-5}	0.086	0.2576	0.0380	-0.2177	-0.0013	0.00034	2.4

[a]1 = NIST fibrous-glass blanket (Calibrated Transfer Specimen Lot)

[a]2-5 = Fibrous-glass blanket (from different manufacturers), ordered by thickness (*L*)

[a]6 = Expanded polystyrene, molded beads

[a]7 = Composite board (expanded polystyrene, plastic facers)

List of Figure Captions

Fig. 1a – Guarded-hot-plate schematic, double-sided mode of operation (vertical heat)

Fig. 1b – Guarded-hot-plate schematic, single-sided mode of operation (heat flow up)

Fig. 2 – NIST 1016 mm Guarded-Hot-Plate Apparatus (horizontal plate configuration)

Fig. 3 – Individual uncertainty contributions for $|c_Q u(Q)|$, $|c_{\Delta T} u(\Delta T)|$, and $|c_A u(A)|$ as a function of specimen heat flow (Q). Predicted curves computed using uncertainty contributions from Equation (11).

Fig. 4 – Expanded uncertainty for thermal resistance ($U(R)$) at 297 K as a function of specimen heat flow and specimen heat flux. Predicted curves computed using Equation (11).

Fig. 5 – Expanded uncertainty for thermal conductivity ($U(\lambda)$) at 297 K as a function of specimen heat flow and specimen heat flux. Predicted curves computed using Equation (13).
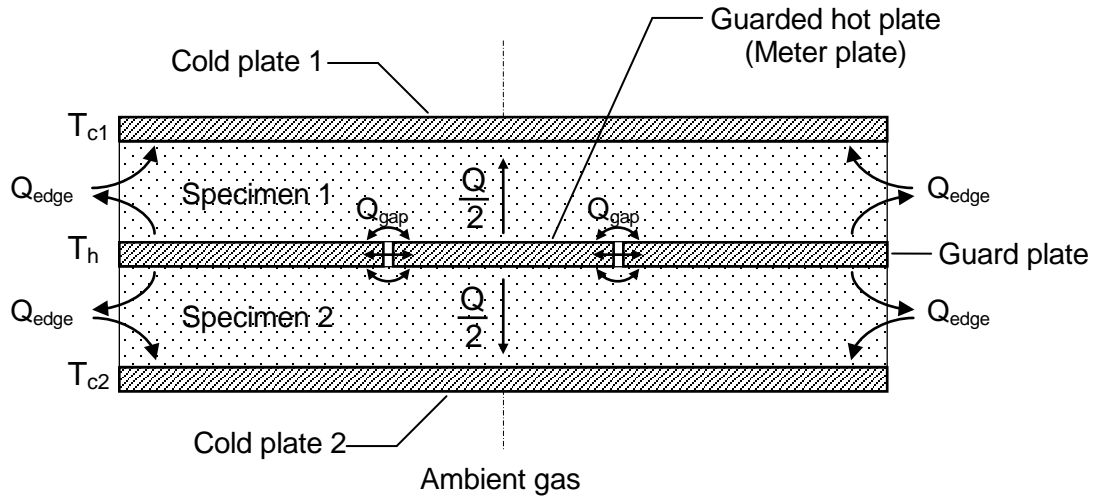
1. Principle: $T_c < T_h$; $T_{c1} = T_{c2} = T_c$
2. Practice: $T_c < T_h$; $T_{c1} \approx T_{c2} \approx T_c$
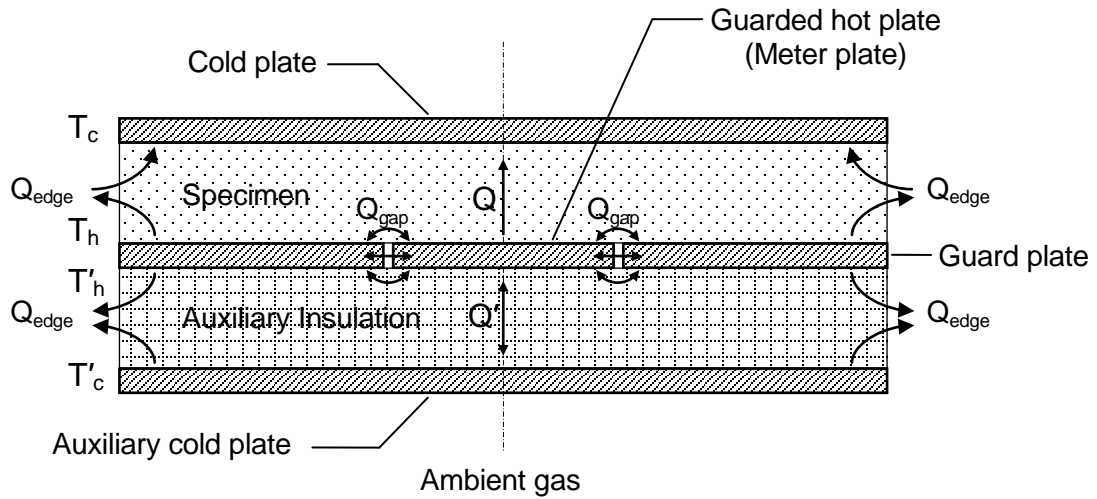
1. Principle: $T_c < T_h$; $T_h = T'_h = T'_c$; $Q' = 0$
2. Practice: $T_c < T_h$; $T_h \approx T'_h \approx T'_c$; $Q' \approx 0$

Q/A, Wm⁻² —